NASA TECHNICAL NOTE

NASA TN D-8233

NASA TN D-8233

EFFECT OF A SURFACE-TO-GAP TEMPERATURE DISCONTINUITY ON THE HEAT TRANSFER TO REUSABLE SURFACE INSULATION TILE GAPS

David A. Throckmorton

Langley Research Center
Hampton, Va. 23665

NATIONAL AERONAUTICS AND SPACE ADMINISTRATION • WASHINGTON, D. C. • JUNE 1976

1. Report No.	2. Government Accession No.	3. Recipient's Catalog No.
NASA TN D-8233		

4. Title and Subtitle	5. Report Date
EFFECT OF A SURFACE-TO-GAP TEMPERATURE DISCONTINUITY ON THE HEAT TRANSFER TO REUSABLE SURFACE INSULATION TILE GAPS	June 1976
	6. Performing Organization Code

7. Author(s)	8. Performing Organization Report No.
David A. Throckmorton	L-10766
	10. Work Unit No.
9. Performing Organization Name and Address	506-26-30-03
NASA Langley Research Center Hampton, Va. 23665	11. Contract or Grant No.
	13. Type of Report and Period Covered
12. Sponsoring Agency Name and Address	Technical Note
National Aeronautics and Space Administration Washington, D.C. 20546	14. Sponsoring Agency Code

15. Supplementary Notes

16. Abstract

An experimental investigation was performed to determine the effect of a surface-to-gap wall temperature discontinuity on the heat transfer within space shuttle, reusable surface insulation (RSI), tile gaps submerged in a thick turbulent boundary layer. Heat-transfer measurements were obtained on a flat-plate, single-gap model submerged in a turbulent tunnel wall boundary layer at a nominal free-stream Mach number of 10.3 and free-stream Reynolds numbers per meter of 1.5×10^6, 3.3×10^6, and 7.8×10^6. Surface-to-gap wall temperature discontinuities of varying degree were created by heating the surface of the model upstream of the instrumented gap. The sweep angle of the gap was varied between 0° and 60°; gap width and depth were held constant.

A surface-to-gap wall temperature discontinuity (surface temperature greater than gap wall temperature) results in increased heat transfer to the near-surface portion of the gap, as compared with the heat transfer under isothermal conditions, while decreasing the heat transfer to the deeper portions of the gap. The nondimensionalized heat transfer to the near-surface portion of the gap was found to decrease with increasing Reynolds number; in the deeper portion of the gap, the heat transfer increased with Reynolds number.

17. Key Words (Suggested by Author(s))

Thermal protection system
Reusable surface insulation
Space shuttle
Gap heating
Boundary layers

18. Distribution Statement

Unclassified – Unlimited

Subject Category 34

19. Security Classif. (of this report)	20. Security Classif. (of this page)	21. No. of Pages	22. Price*
Unclassified	Unclassified	34	$3.75

*For sale by the National Technical Information Service, Springfield, Virginia 22161

EFFECT OF A SURFACE-TO-GAP TEMPERATURE DISCONTINUITY ON THE HEAT TRANSFER TO REUSABLE SURFACE INSULATION TILE GAPS

David A. Throckmorton
Langley Research Center

SUMMARY

An experimental investigation was performed to determine the effect of a surface-to-gap wall temperature discontinuity on the heat transfer within space shuttle, reusable surface insulation (RSI), tile gaps submerged in a thick turbulent boundary layer. Heat-transfer measurements were obtained on a flat-plate, single-gap model submerged in a turbulent tunnel wall boundary layer at a nominal free-stream Mach number of 10.3 and free-stream Reynolds numbers per meter of 1.5×10^6, 3.3×10^6, and 7.8×10^6. Surface-to-gap wall temperature discontinuities of varying degree were created by heating the surface of the model upstream of the instrumented gap. The sweep angle of the gap was varied between 0° and 60°; gap width and depth were held constant.

A surface-to-gap wall temperature discontinuity (surface temperature greater than gap wall temperature) results in increased heat transfer to the near-surface portion of the gap, as compared with the heat transfer under isothermal conditions, while decreasing the heat transfer to the deeper portions of the gap. The nondimensionalized heat transfer to the near-surface portion of the gap was found to decrease with increasing Reynolds number; in the deeper portion of the gap, the heat transfer increased with Reynolds number.

INTRODUCTION

The space shuttle orbiter thermal protection system (TPS) will be a surface covering of a nonmetallic, low-density, refractory oxide. This material, referred to as reusable surface insulation (RSI), is capable of withstanding repeated exposure to the reentry environment while insulating the vehicle structure from surface temperatures in excess of 1500 K. The material is attached to the vehicle surface in a bricklike array of square tiles (15.25 cm by 15.25 cm) which vary in thickness from about 1 to 10 centimeters according to the intensity of the local heating. Small gaps between tiles accommodate thermal expansion and contraction and other deflections of the underlying structure and

also allow for thermal expansion of the tile material. Effective design of the TPS requires a sound knowledge of the aerodynamic heating environment to which the RSI tiles are subjected. This knowledge must include an accurate definition of the heat-transfer distribution within the tile gaps and a good understanding of how this distribution is affected by changes in the external boundary layer and tile-surface-condition variations.

As a part of the space shuttle development program, an experimental effort has been focused on the shuttle-related gap heating problems. Tests have previously been conducted to assess the effects on the tile heat transfer of gap width, gap edge radius, gap orientation, gap intersections, tile surface mismatch, boundary-layer state (laminar/turbulent), boundary-layer thickness, and surface pressure gradient. Results of some of these investigations are reported in references 1 to 6. Each of these investigations has contributed to better definition of the gap heating to an RSI tile array. However, all these tests were conducted with models initially at an isothermal condition. Because convective heating rates within the tile gaps have been shown to be substantially lower than those to the tile exterior surface, flight wall temperatures within the gaps are similarly expected to be substantially lower than tile exterior surface temperature. None of the previous tests simulated this nonisothermal condition. The present investigation was conducted to assess the effects of a tile exterior-to-gap temperature "discontinuity" on the heat transfer to the tile gap wall in a thick turbulent boundary layer. Simulation of the nonisothermal condition was achieved by electrically heating a surface plate upstream of a thermally isolated, instrumented gap. The results of this investigation should then allow more accurate application of isothermal test data for extrapolation to flight conditions.

Heat-transfer tests were made on a single-gap model submerged in a thick turbulent tunnel sidewall boundary layer. The model was tested at free-stream unit Reynolds numbers per meter of 1.5×10^6, 3.3×10^6, and 7.8×10^6; the free-stream Mach number was 10.3. Ratios of heated-plate surface temperature to gap-wall temperature were nominally 1.0, 1.2, 1.4, and 1.6. Gap sweep angle was varied from 0^o (transverse to the flow direction) to 60^o.

SYMBOLS

$c_{p,m}$	specific heat of model material, J/kg-K
h	heat-transfer coefficient, W/m^2-K
N_{St}	Stanton number
q	heat-transfer rate, W/m^2

$R_{w,\theta}$	Reynolds number based on wall conditions and boundary-layer momentum thickness
R_∞	free-stream Reynolds number, m^{-1}
r	recovery factor
T	temperature, K
t	time, sec
w	gap width, cm
z	depth into gap, cm
δ^*	boundary-layer displacement thickness, cm
θ	boundary-layer momentum thickness, cm
Λ	gap sweep angle, deg
λ_m	model material thickness, m
ρ_m	model material density, kg/m^3

Subscripts:

aw	adiabatic wall
fp	flat plate
gap	gap wall
surf	heated plate surface
t	total
w	local wall
∞	free stream

APPARATUS AND TESTS

Facility

The experimental results presented herein were obtained in the Langley continuous-flow hypersonic tunnel. This facility, which has a 78.74-cm-square test section, operates at a nominal free-stream Mach number of 10.3 over a range of Reynolds number per meter of 1.5×10^6 to 8.2×10^6 using air as the test gas, and may be operated in either a blowdown or continuous, closed-circuit mode. To prevent liquefaction, the air is heated by means of an electrical resistance tube bundle. The tunnel throat, expansion, and diffuser sections are all water cooled.

For these tests, the model was mounted on the facility model injection mechanism adjacent to the test section. This device allows a model to be isolated from the hypersonic airstream for model cooling or configuration changes while the tunnel is operating. The mechanism also provides rapid injection of a model into the hypersonic airstream for the purpose of transient heating.

Model

The model consisted of a smooth heated plate upstream of a thermally isolated, instrumented, thin-skin gap. A schematic drawing of the model is shown in figure 1. The forward surface plate was fabricated from 0.3175-cm-thick brass and could be heated by an array of four electrical resistance heaters (one 350 W heater, and three 400 W heaters) attached to the backside of the plate. The heated plate was instrumented with 15 chromel-alumel thermocouples, equally spaced in three arrays (fig. 2), to record bulk plate temperature. The rear surface plate was fabricated from 17-4 PH stainless steel and was not heated or instrumented.

The thin-skin gap, formed from 0.0406-cm type 304 stainless-steel sheet, was 0.229 cm wide and 4.572 cm deep. The gap was thermally isolated from the heated plate by means of a thermal insulator and a water-cooling passage. At its midspan, the gap was instrumented with 21 30-gage chromel-alumel thermocouples spotwelded to the backface of the gap walls (both upstream and downstream) at locations indicated in figure 2.

The entire model assembly, gap and surface plates, fit within an adapter plate to the tunnel model injection system. The adapter allowed the model surface to lie flush with the injection plate; thus, it became an integral part of the tunnel sidewall during testing. The adapter plate was rotatable so that the gap could be tested at any sweep angle with respect to the flow. All thermocouples within the gap were located at the rotation center.

Figure 3 is a photograph of the model mounted on the facility injection mechanism ready for testing.

Test Procedures and Conditions

The transient-calorimeter technique was used to determine heat-transfer rates to the surface of the thin-skin gap. The model was initially isolated from the hypersonic airstream, within the injection chamber, at a pressure equal to the test-section static pressure. With the hypersonic flow established in the test section, the heated plate was brought up to the desired temperature level. At this point, the heaters and gap cooling were turned off; and the model was rapidly injected to the test position, flush with the tunnel sidewall. Temperature data were automatically recorded on magnetic tape by an analog-to-digital converter at a rate of 20 samples per second for a period of about 5 seconds, after which the model was retracted from the test position.

The model was tested at total pressures in the settling chamber of 2.41, 5.34, and 12.07 MN/m^2, corresponding to nominal free-stream unit Reynolds numbers per meter of 1.5×10^6, 3.3×10^6, and 7.8×10^6. Measured velocity profiles, and momentum and displacement thicknesses for this tunnel wall boundary layer are reported in reference 6. The momentum and displacement thicknesses at the model center of rotation (gap thermocouple location) are shown in figure 4. Ratios of heated-plate surface temperature to gap-wall temperature T_{surf}/T_{gap} were nominally 1.0, 1.2, 1.4, and 1.6. Local temperature of the heated plate upstream of the gap was always within ±3 percent of the mean. Gap sweep angle Λ was varied between 0^o (transverse to the flow direction) and 60^o.

Data Reduction

The test procedure of rapid injection of the isothermal (within the instrumented gap) model to the test position provided a step input in heat transfer to the thin-skin gap. Heat-transfer rates were determined by the transient calorimeter technique of measuring the time rate of change of the model skin temperature. For data-reduction purposes, the one-half second interval of temperature data immediately following model injection was disregarded to allow flow conditions to stabilize in the gap. This time is in excess of that required for diffusion of vorticity and heat into the gap, as reported by Nicoll. (See ref. 7.) A quadratic curve was fitted, by the method of least squares, to the subsequent 3-second interval of data for each thermocouple. The long interval (3 seconds) of temperature-time data used for heat-transfer rate calculation allowed measurement of the low heating rates found within the gaps which were not readily discernible when a shorter interval (1 second) of data was considered. An assessment of conduction effects which resulted from the long data interval, for representative data from this test, indicates a maximum error in computed heating rate of less than 10 percent. Rates of change of

temperature with time $\partial T_w/\partial t$ were evaluated analytically from the curve-fit expressions at the initial point of each curve fit. Heat-transfer rates were then computed from the expression

$$q = \rho_m c_{p,m} \lambda_m \frac{\partial T_w}{\partial t}$$

Heat-transfer data are expressed in the form of the heat-transfer coefficient h defined as

$$h = \frac{q}{T_{aw} - T_w}$$

Adiabatic wall temperature T_{aw} was computed from the expression

$$r = \frac{T_{aw} - T_\infty}{T_t - T_\infty}$$

where recovery factor r was assumed equal to 0.89 for the turbulent test conditions.

RESULTS AND DISCUSSION

Basic Data

Measured heat-transfer coefficients to the upstream and downstream walls of the instrumented gap are presented in figures 5 to 7 for all conditions of temperature ratio, Reynolds number, and sweep angle of the tests. The data are nondimensionalized by the heat-transfer coefficient measured on a smooth flat plate on the tunnel sidewall at the location of the instrumented gap. (See appendix.) The temperature of the flat-plate reference model (isothermal) corresponds to a surface-to-gap wall temperature ratio T_{surf}/T_{gap} of 1.0. The solid symbols in these, and all additional figures, indicate extremely low heat-transfer-rate data which are of questionable accuracy. These data are included for completeness.

In all cases tested, the heat-transfer coefficient decreases with increasing depth into the gap for both the upstream and downstream gap walls. Heat transfer to the downstream gap wall, however, is always higher than that to the upstream gap wall for depths into the gap of less than four gap widths ($z/w < 4$). The higher downstream wall heat transfer results from impingement on the downstream wall of a shear layer which emanates from the upstream gap corner. At locations deeper within the gap ($z/w > 5$),

heating rates to the upstream and downstream walls are approximately equal. At the lowest Reynolds number, increasing the surface-to-gap wall temperature ratio magnifies the difference between downstream and upstream gap-wall heat transfer. This effect, however, is not so evident at the higher Reynolds numbers.

A comparison of data for the three values of sweep angle at a single Reynolds number and temperature ratio indicates a negligible effect of sweep on gap heat transfer over the range of sweep angle of the tests. If sweep angle were increased, the gap orientation would change from transverse to the flow direction to parallel to the flow direction as the sweep angle approached 90°. At $\Lambda = 90^{\circ}$, heating to both gap walls would be expected to become equal at a level between those experienced by the upstream and downstream walls at some lesser sweep angle. The range of sweep angle considered in these tests was insufficient to obtain data which would illustrate this trend. Therefore, the effects of gap sweep angle on gap heat transfer are not discussed further.

Effects of Surface-to-Gap Wall Temperature Ratio

The effect of a variable surface-to-gap wall temperature ratio on downstream gap-wall heating is illustrated in figure 8. This figure contains the basic gap data and a downstream surface data point at all surface-to-gap wall temperature ratios, superimposed for each Reynolds number and sweep angle of the tests. Increasing the surface-to-gap wall temperature ratio above 1.0 tends to increase the heat transfer to the near-surface portion of the gap, while slightly decreasing the heat transfer in the deeper part of the gap. The reversal in trend with surface-to-gap wall temperature ratio generally occurs at a depth into the gap of between two and three gap widths ($2 < z/w < 3$). The faired data of figure 8(a), $\Lambda = 0^{\circ}$, are plotted in figure 9 as a function of T_{surf}/T_{gap} for several values of z/w to illustrate more clearly the effect of the nonisothermal condition.

The phenomenon of increased heating to the near-surface portion of the gap, due to the temperature discontinuity, is characteristic of any boundary-layer flow over a surface which has a similar step decrease in wall temperature. (See ref. 8.) A step change in wall temperature causes a spatially instantaneous change in the boundary-layer temperature distribution near the wall and, therefore, a change in the fluid temperature gradient at the wall. Since heat transfer is directly dependent on the fluid temperature gradient at the wall, any mechanism which affects this gradient also affects heat transfer. In this manner, a step increase in wall temperature will result in decreased heat transfer downstream of the temperature step, and, conversely, a step decrease in wall temperature will result in increased heat transfer downstream as was observed in the present test. The decreased heat transfer with T_{surf}/T_{gap} observed deep in the gap ($z/w > 3$) is attributed to a loss of energy in the gap flow available for heat transfer at these depths as a result of the increased heating to the gap near the surface.

Effects of Reynolds Number

The variation of downstream gap-wall heating with free-stream unit Reynolds number is illustrated in figure 10 for $\Lambda = 0^{\circ}$. Increasing unit Reynolds number reduces the nondimensional heat transfer near the top of the gap ($z/w < 2$), while increasing the heat transfer in the deeper portion of the gap ($z/w > 3$). The decrease in near-surface nondimensional heat transfer is attributed to Reynolds number dependent changes in the character of the flow separation across the gap. Increased in-depth heating probably results from increased diffusion of high energy flow deeper into the gap as a result of the increasing Reynolds number.

The trends of heat transfer with Reynolds number R_{∞} are opposite to those which have been shown for the temperature ratio T_{surf}/T_{gap}. As Reynolds number increases, the impact of nonisothermal temperature conditions on gap heat transfer is lessened.

Flight Temperature and Boundary-Layer Simulation

A comparison of the surface-to-gap wall temperature ratios of these tests with those expected in flight is presented in figure 11. The predicted flight temperatures (based on unpublished data furnished by L. H. Ebbesmeyer and H. E. Christensen of McDonnell-Douglas Astronautics Co.) are for a lower surface body point near the vehicle nose, when the vehicle is at the peak heating point of a typical entry trajectory. The temperatures result from an analysis of the thermal response of the shuttle TPS material to a gap heating distribution which is a correlation of previously measured isothermal model data. (See ref. 4.) The data resulting from the present test program were obtained at temperature discontinuity conditions more severe than expected in flight, and at temperature ratios which span fully those predicted for the flight case.

Reference 4 indicates that although the boundary-layer edge Mach number and unit Reynolds numbers of the present tests are higher than those expected in flight, the boundary-layer displacement and momentum thicknesses provide good simulation for a range of flight body-point and trajectory-point combinations.

CONCLUDING REMARKS

An experimental investigation has been conducted to assess the effect of a surface-to-gap wall temperature discontinuity on the heat transfer to reusable surface insulation tile gaps submerged in a thick turbulent boundary layer. The experimental program consisted of heat-transfer measurements on a single, simulated tile gap in the tunnel-wall boundary layer of the Langley continuous-flow hypersonic tunnel for a range of free-stream Reynolds numbers, gap sweep angles, and surface-to-gap wall temperature ratios.

Simulation of surface-to-gap wall temperature ratios expected for a reusable surface insulation tile in flight was good although the temperature discontinuity produced for these tests was more severe than will be experienced in flight.

A surface-to-gap wall temperature discontinuity $\left(T_{surf} > T_{gap}\right)$ results in increased heating to the near-surface portion of the gap, as compared with the heat transfer under isothermal conditions. The magnitude of the heating increase is directly proportional to the surface-to-gap wall temperature ratio. However, at depths within the gap in excess of three (3) gap widths, heat transfer tends to decrease with an increasing surface-to-gap wall temperature ratio. This decrease is attributed to a loss of energy in the gap flow at these depths as a result of the increased heating to the gap near the surface.

Nondimensionalized heat transfer to the near-surface portion of the gap was found to decrease with increasing Reynolds number. This phenomenon is attributed to Reynolds number dependent changes in the character of the flow separation across the gap. Increasing Reynolds number resulted in increased nondimensional heat transfer to that portion of the gap more than three (3) gap widths from the surface.

Heat transfer to the upstream gap wall was always lower than that to the downstream gap wall for depths into the gap of less than four (4) gap widths. At locations deeper within the gap, heating rates to the upstream and downstream walls were approximately equal.

Langley Research Center
National Aeronautics and Space Administration
Hampton, Va. 23665
April 15, 1976

APPENDIX

SURFACE REFERENCE HEAT TRANSFER

Measured heat transfer to a smooth flat plate mounted in the sidewall of the Langley continuous-flow hypersonic tunnel is presented in reference 6. These data were shown to correlate as

$$N_{St} R_{w,\theta}^{0.07} = \text{Constant} \tag{A1}$$

For the purpose of the present investigation, the correlation of flat-plate heating presented in reference 6 was reduced to the form

$$h_{fp} \propto R_{\infty}^{0.69} \tag{A2}$$

Comparison of the measured data and this correlation equation (A2) is shown in the following figure. All data presented in this report are nondimensionalized by the heat transfer to a smooth flat plate as determined by this correlation expression (A2).

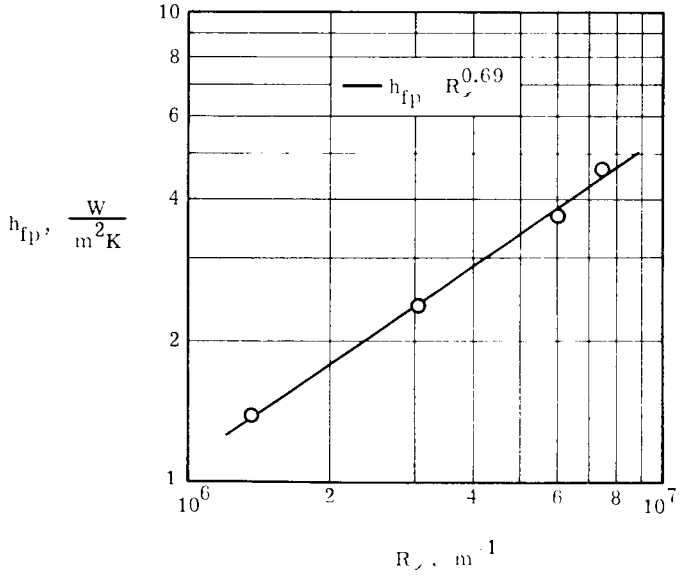

REFERENCES

1. Johnson, Charles B.: Heat Transfer Data to Cavities Between Simulated RSI Tiles at Mach 8. NASA CR-128770, 1973.

2. Foster, Thomas F.; Lockman, William K.; and Grifall, William J.: Thermal Protection System Gap Heating Rates of the Rockwell International Flat Plate Heat Transfer Model (OH2A/OH2B). NASA CR-134077, 1973.

3. Throckmorton, David A.: Heat Transfer to Surface and Gaps of RSI Tile Arrays in Turbulent Flow at Mach 10.3. NASA TM X-71945, 1974.

4. Christensen, H. E.; and Kipp, H. W.: Data Correlation and Analysis of Arc Tunnel and Wind Tunnel Tests of RSI Joints and Gaps. Volume I – Technical Report. NASA CR-134345, 1974.

5. Dunavant, James C.; and Throckmorton, David A.: Aerodynamic Heat Transfer to RSI Tile Surfaces and Gap Intersections. J. Spacecraft & Rockets, vol. 11, no. 6, June 1974, pp. 437-440.

6. Throckmorton, David A.: Pressure Gradient Effects on Heat Transfer to Reusable Surface Insulation Tile-Array Gaps. NASA TN D-7939, 1975.

7. Nicoll, K. M.: Use of Transient "Thin-Wall" Technique in Measuring Heat Transfer Rates in Hypersonic Separated Flows. AIAA J., vol. 1, no. 4, Apr. 1963, pp. 940-941.

8. Rubesin, Morris W.: The Effect of an Arbitrary Surface-Temperature Variation Along a Flat Plate on the Convective Heat Transfer in an Incompressible Turbulent Boundary Layer. NACA TN 2345, 1951.

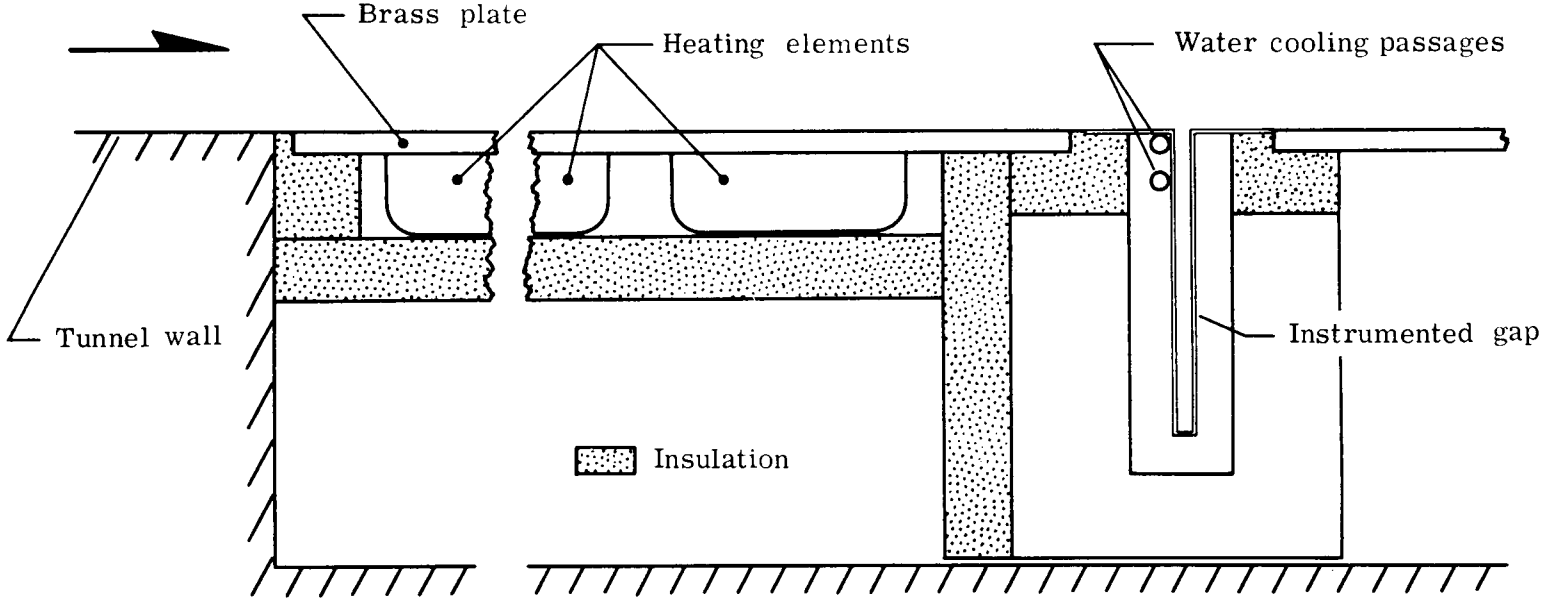

Figure 1. - Nonisothermal gap model schematic.

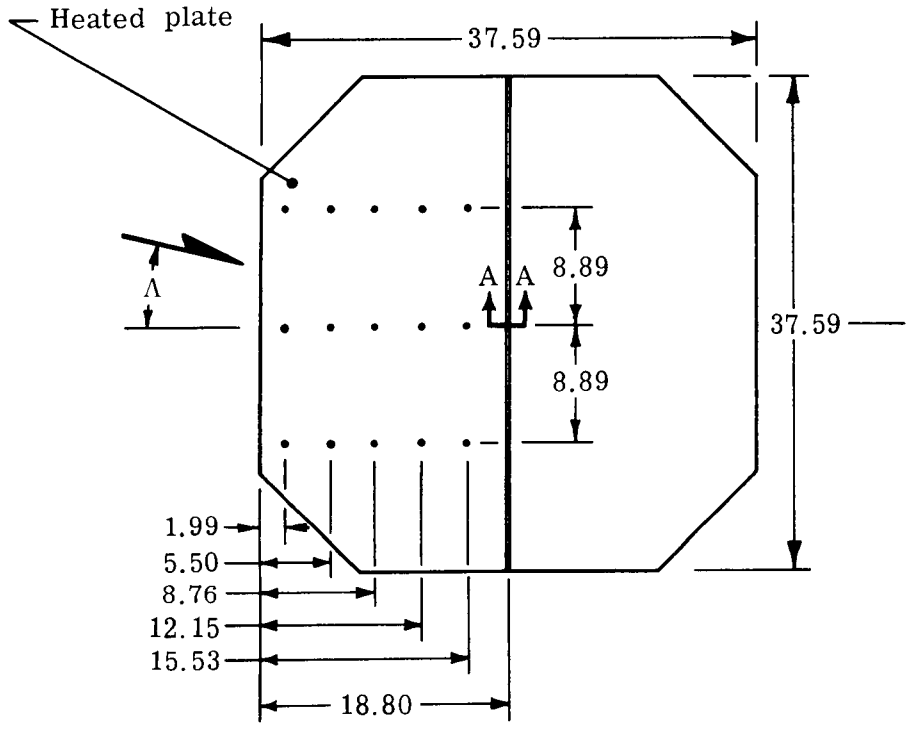

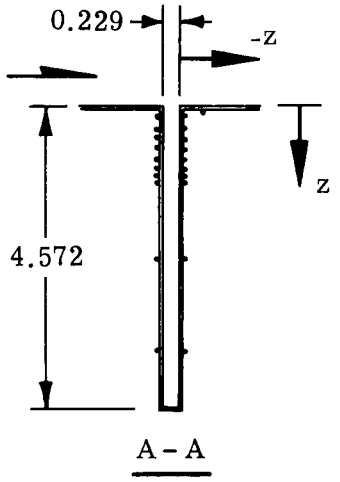

Gap thermocouple locations			
Downstream wall		Upstream wall	
Number	z	Number	z
1	0.160	11	0.160
2	.318	12	.318
3	.475	13	.475
4	.635	14	.635
5	.795	15	.795
6	.953	16	.953
7	1.049	17	1.049
8	1.143	18	1.143
9	2.286	19	2.286
10	3.683	20	3.683
		21	-.318

Figure 2. - Nonisothermal gap model thermocouple locations. All dimensions are in centimeters.

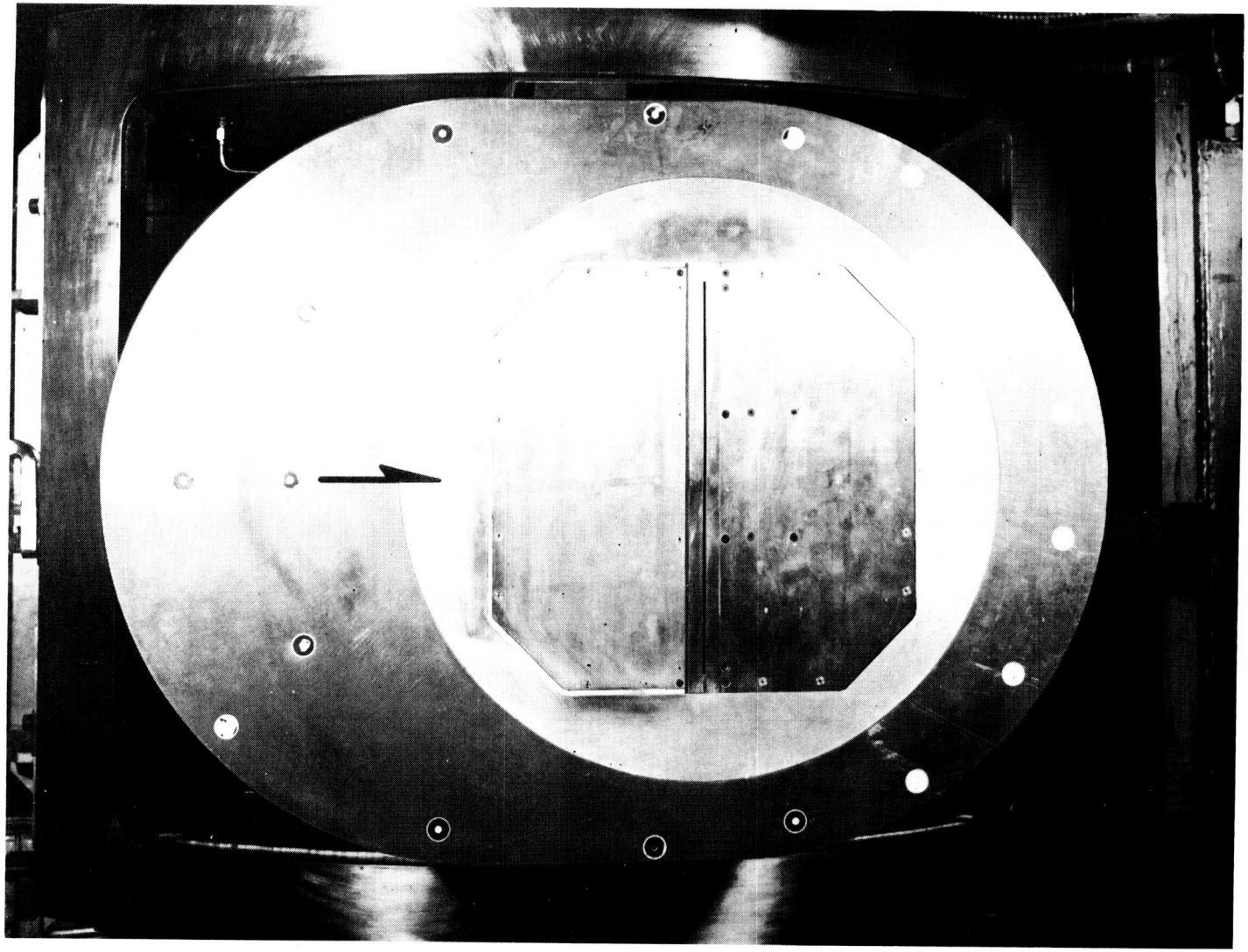

L-74-1338

Figure 3.- Nonisothermal gap model mounted on injection strut. $\Lambda = 0^{o}$.

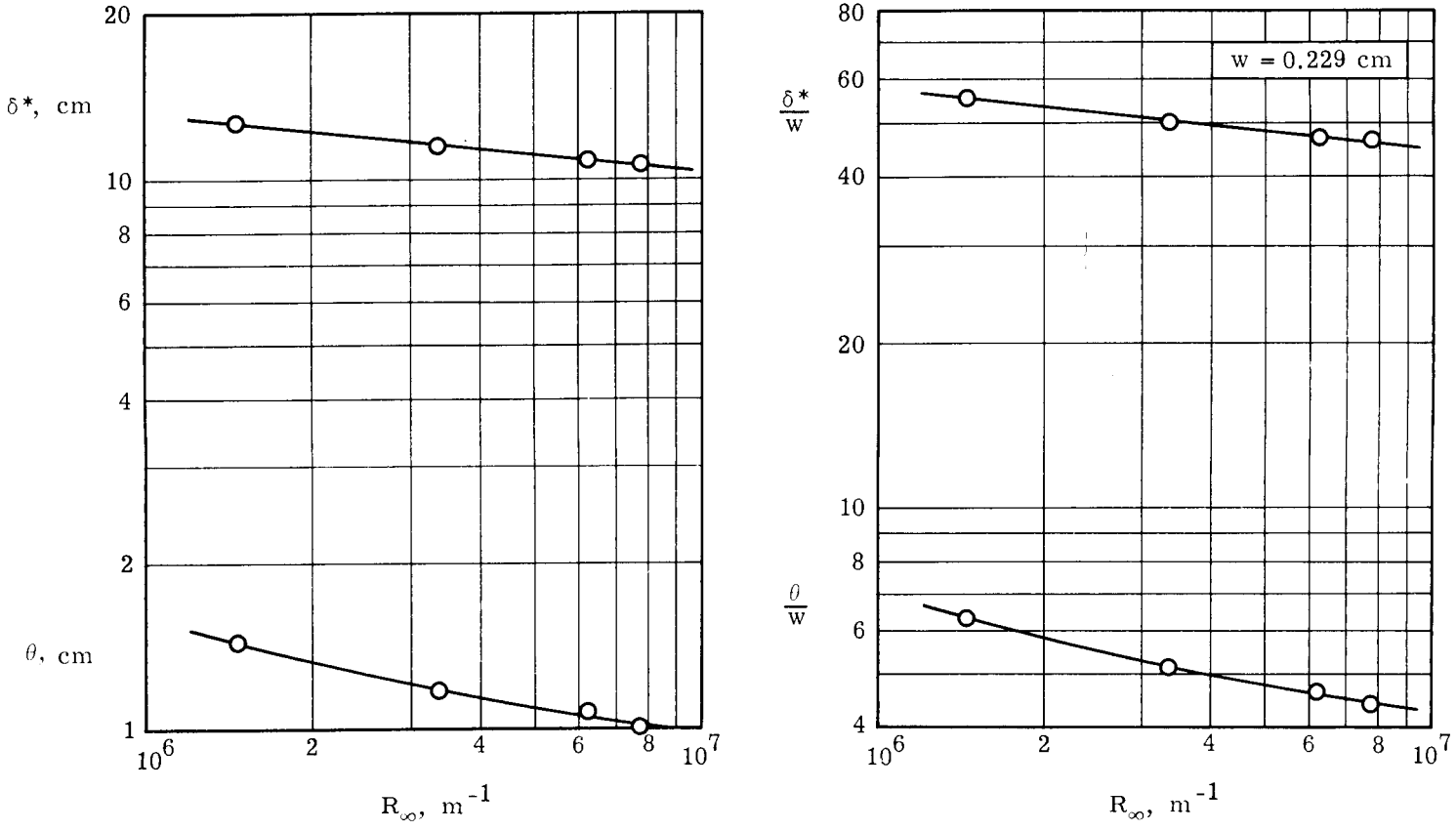

Figure 4. - Variation of wall boundary-layer thickness with free-stream unit Reynolds number.

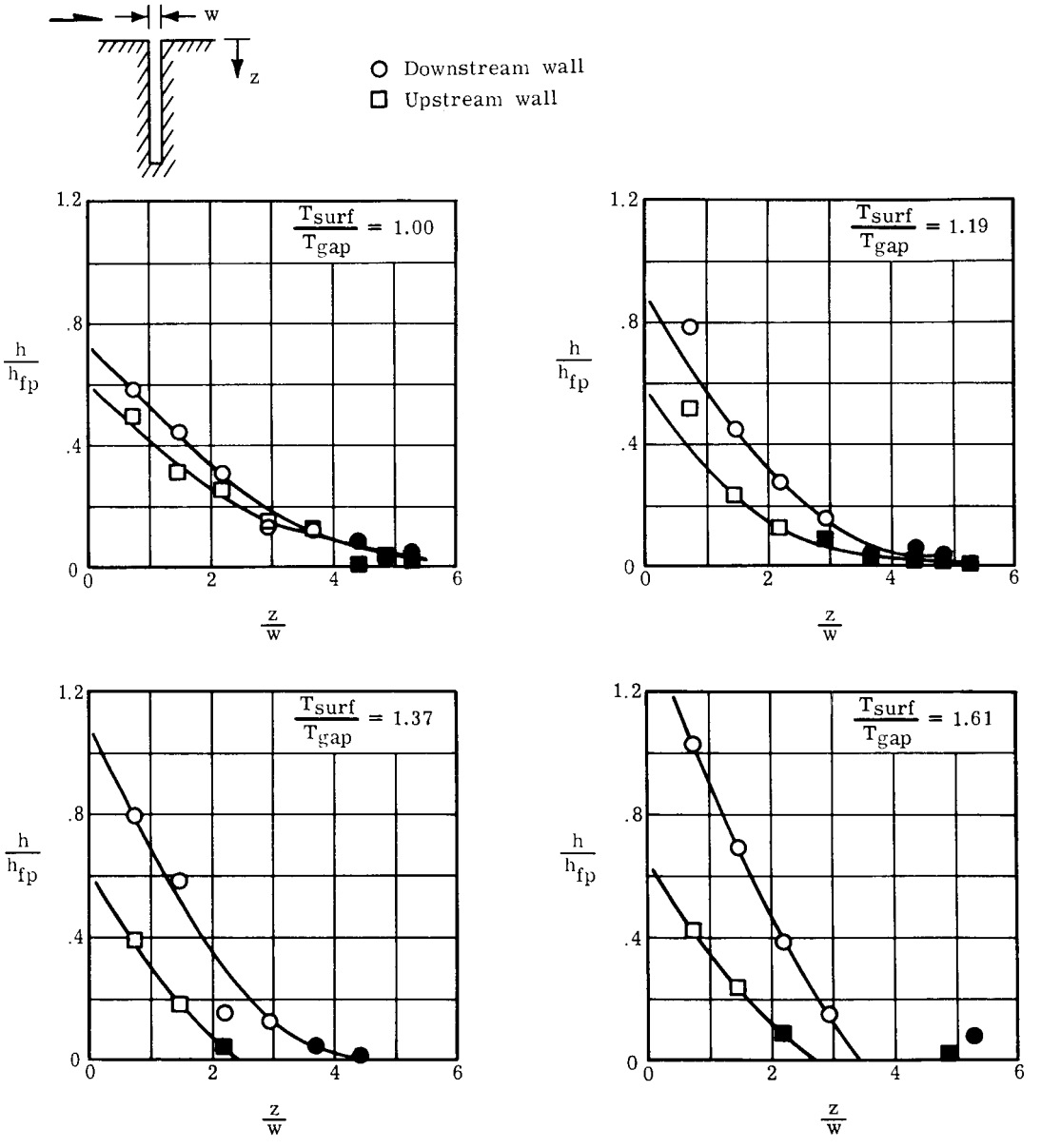

(a) $R_\infty = 1.47 \times 10^6\ m^{-1}$.

Figure 5.- Measured heat transfer within the gap. $\Lambda = 0^o$.

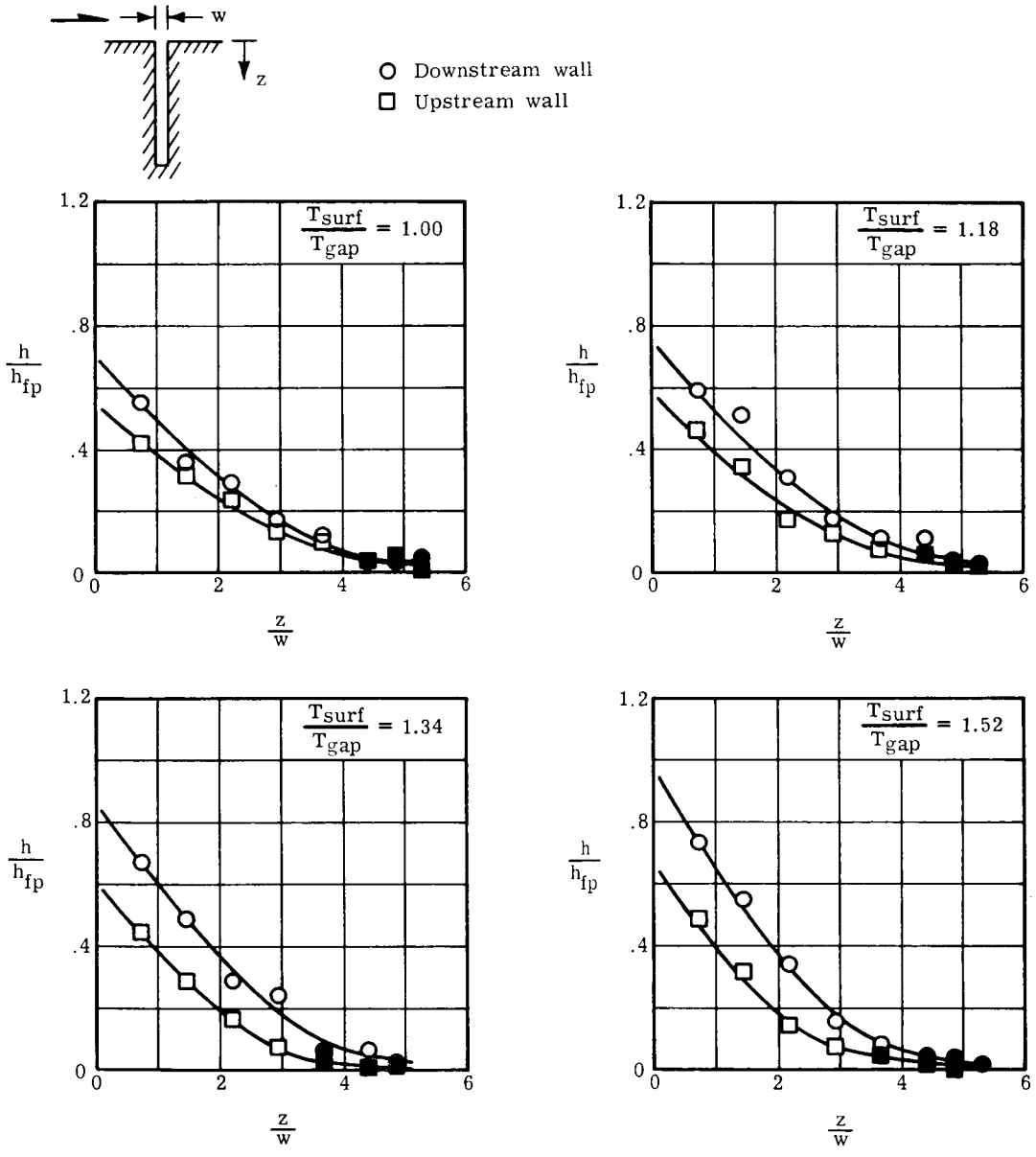

(b) $R_{\infty} = 3.32 \times 10^{6}\ m^{-1}$.

Figure 5.- Continued.

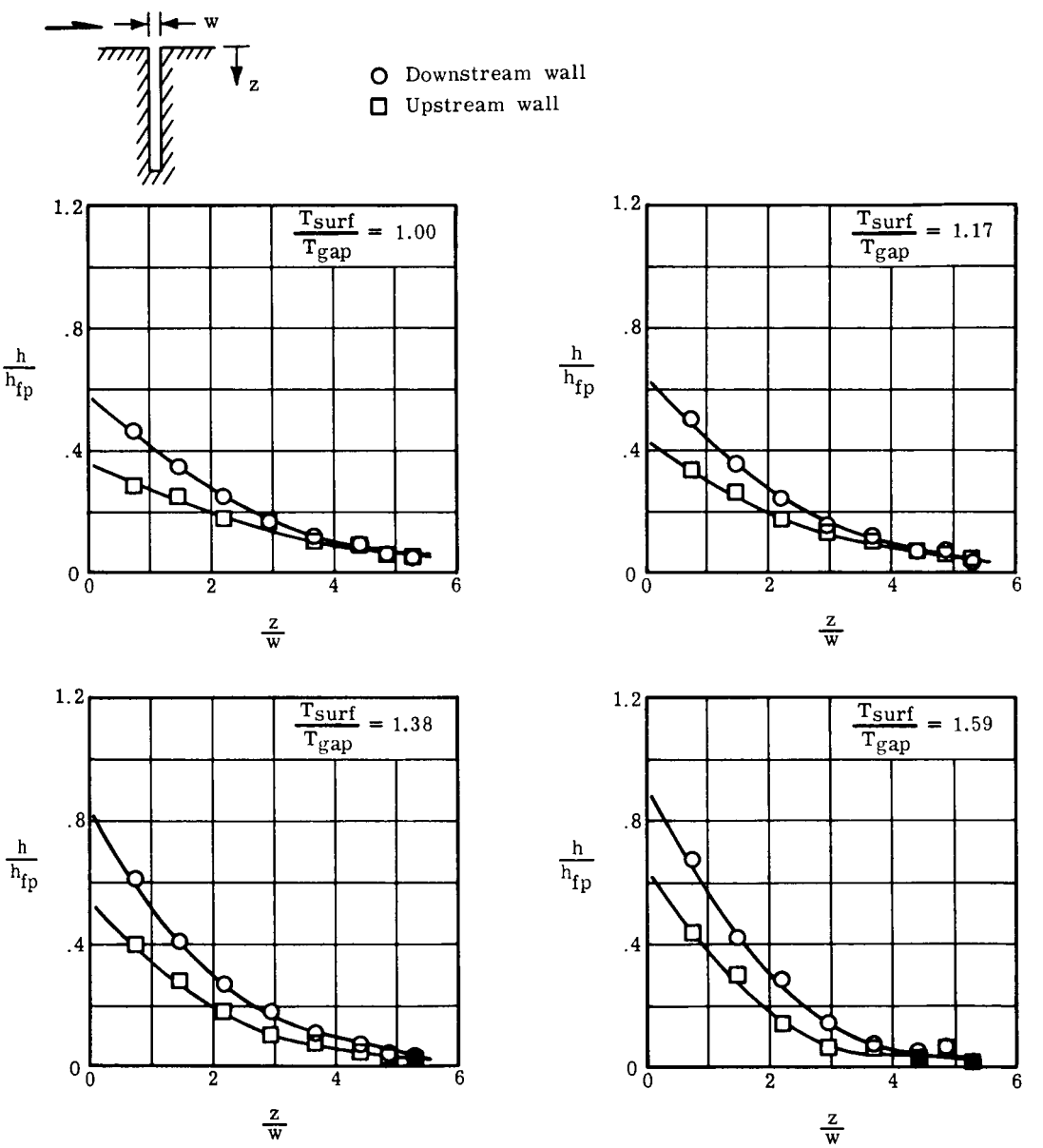

(c) $R_{\infty} = 7.82 \times 10^{6}\ m^{-1}$.

Figure 5.- Concluded.

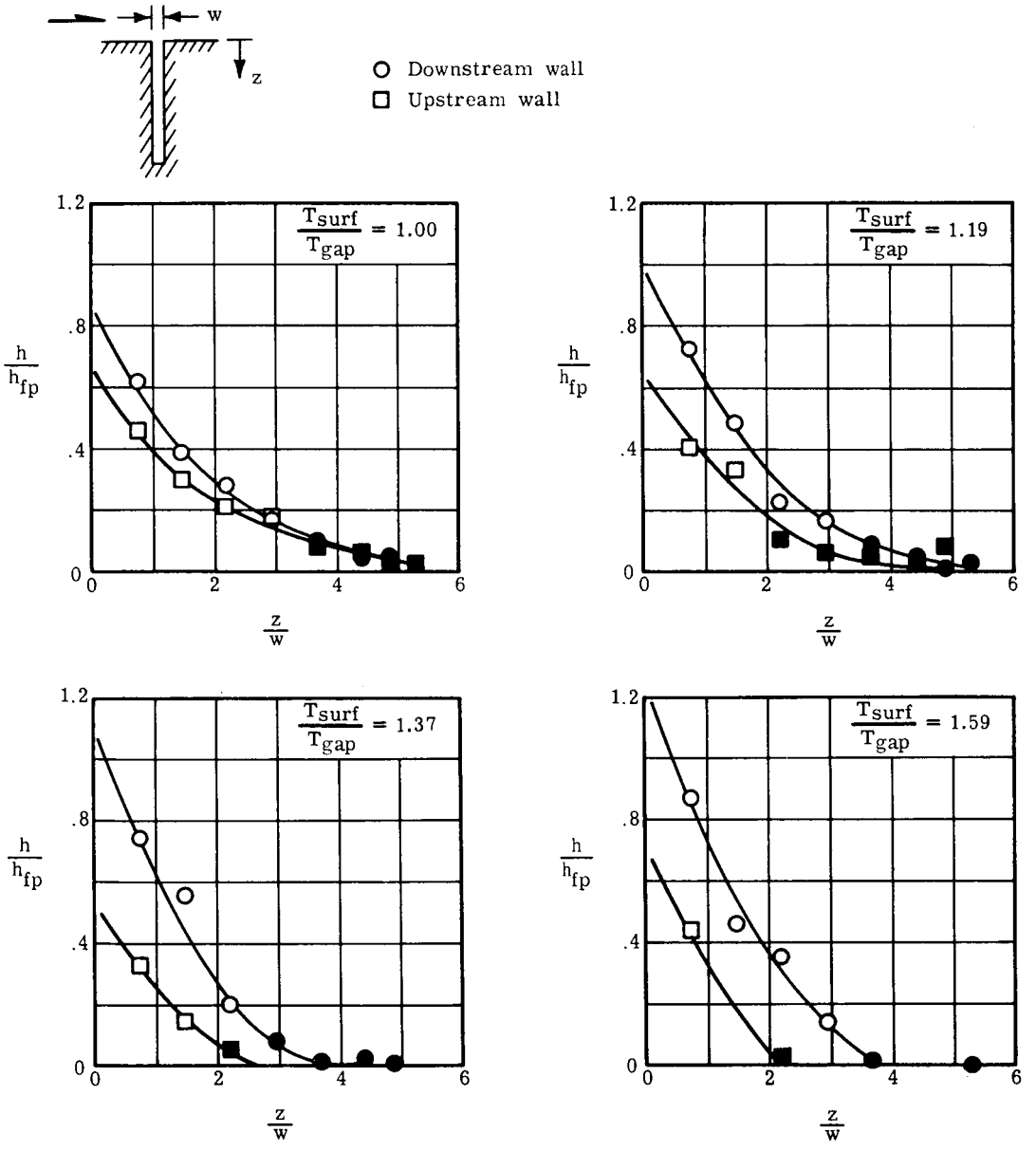

(a) $R_{\infty} = 1.47 \times 10^{6}\ m^{-1}$.

Figure 6.- Measured heat transfer within the gap. $\Lambda = 30^{o}$.

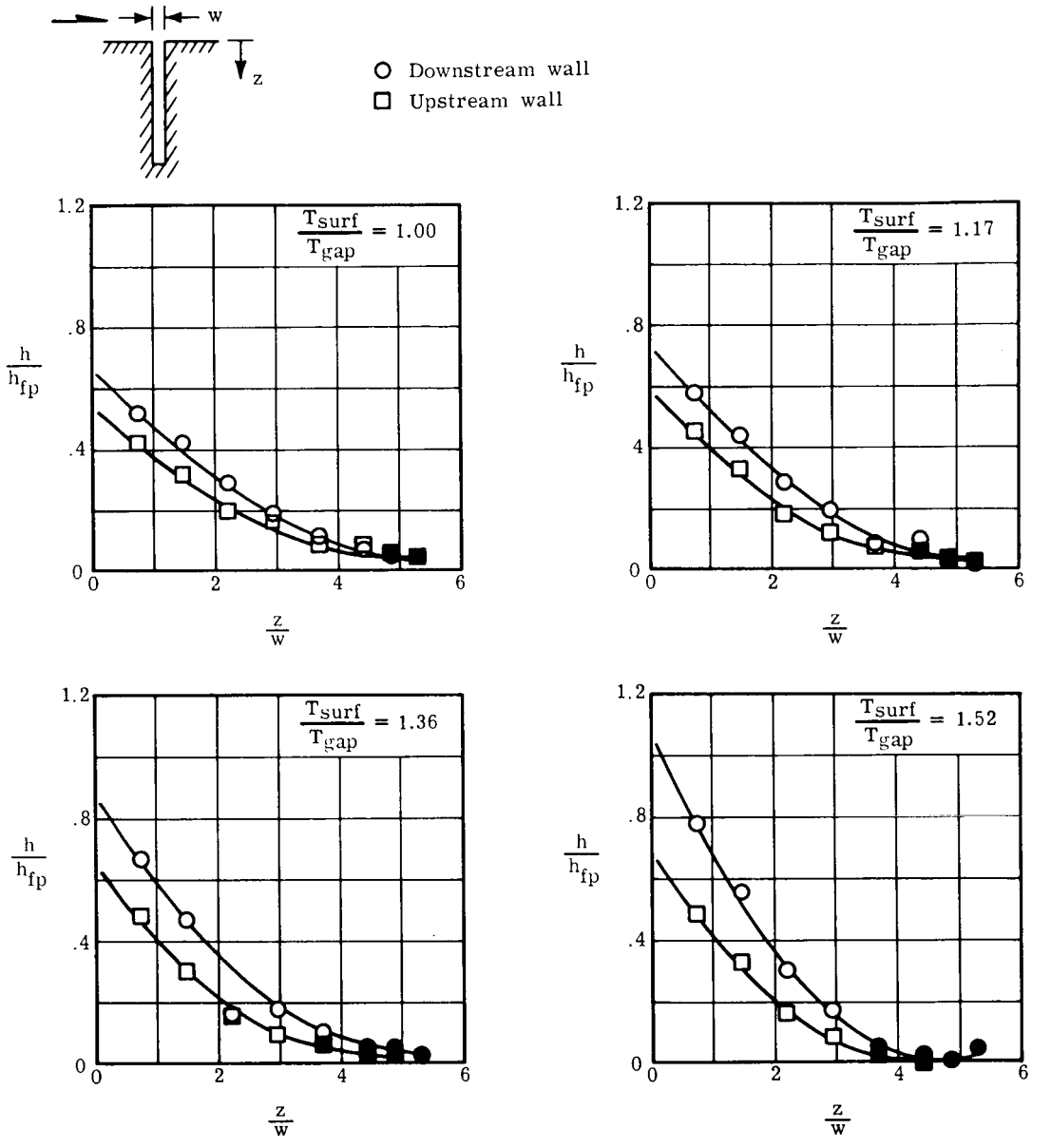

(b) $R_{\infty} = 3.26 \times 10^{6}\ m^{-1}$.

Figure 6.- Continued.

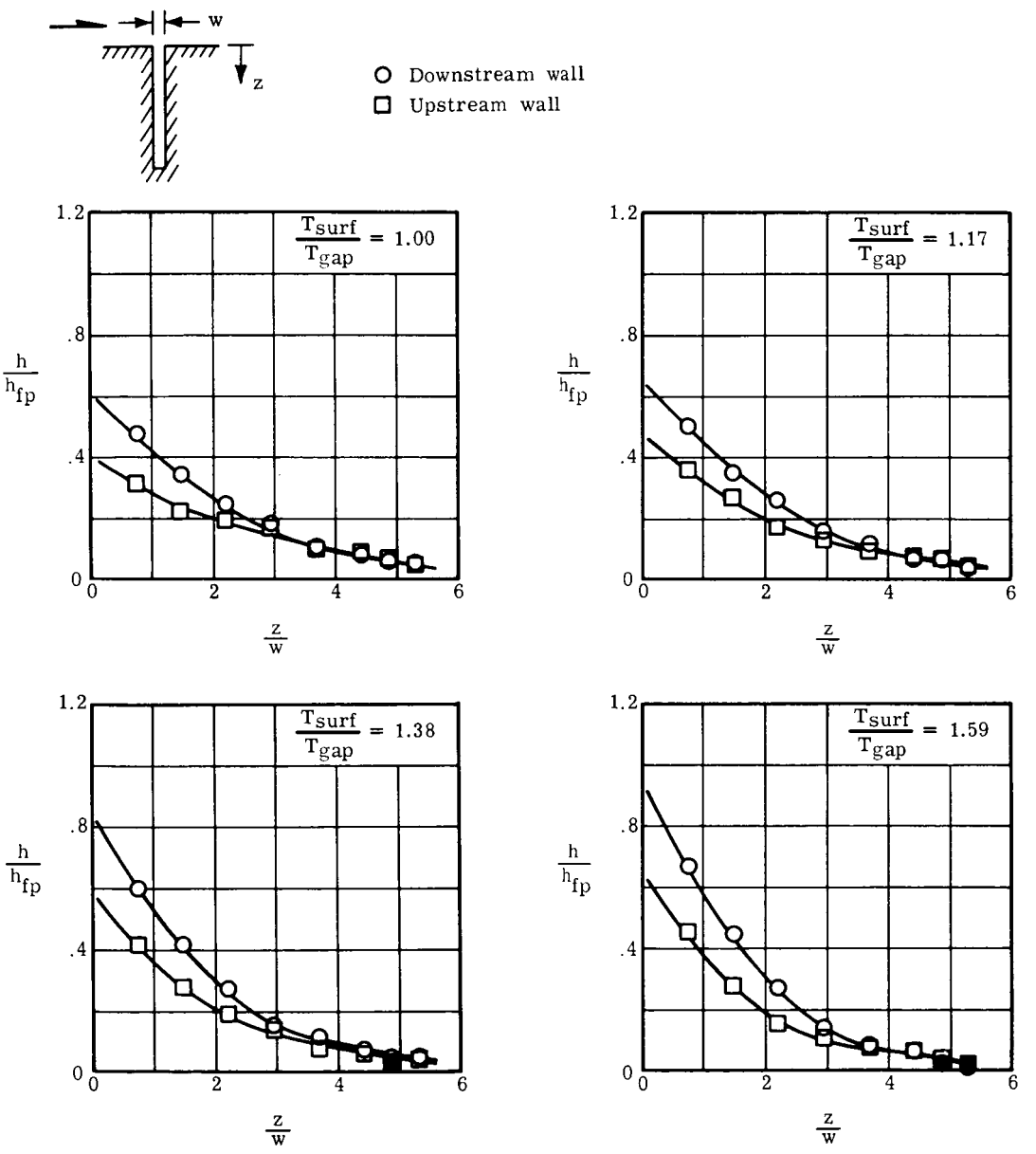

(c) $R_{\infty} = 7.82 \times 10^{6}\ m^{-1}$.

Figure 6.- Concluded.

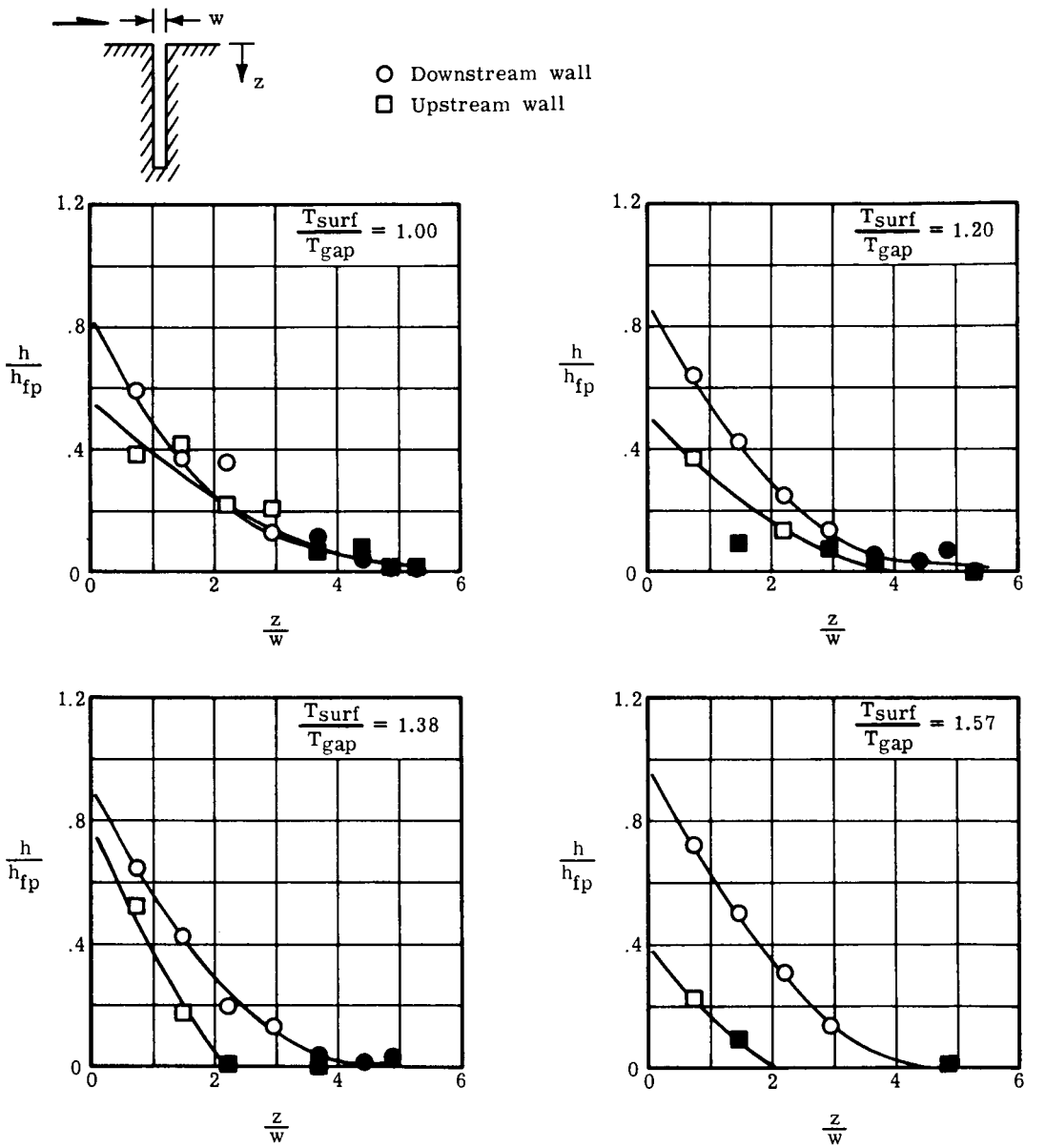

(a) $R_{\infty} = 1.48 \times 10^{6}\ m^{-1}$.

Figure 7.- Measured heat transfer within the gap. $\Lambda = 60^{o}$.

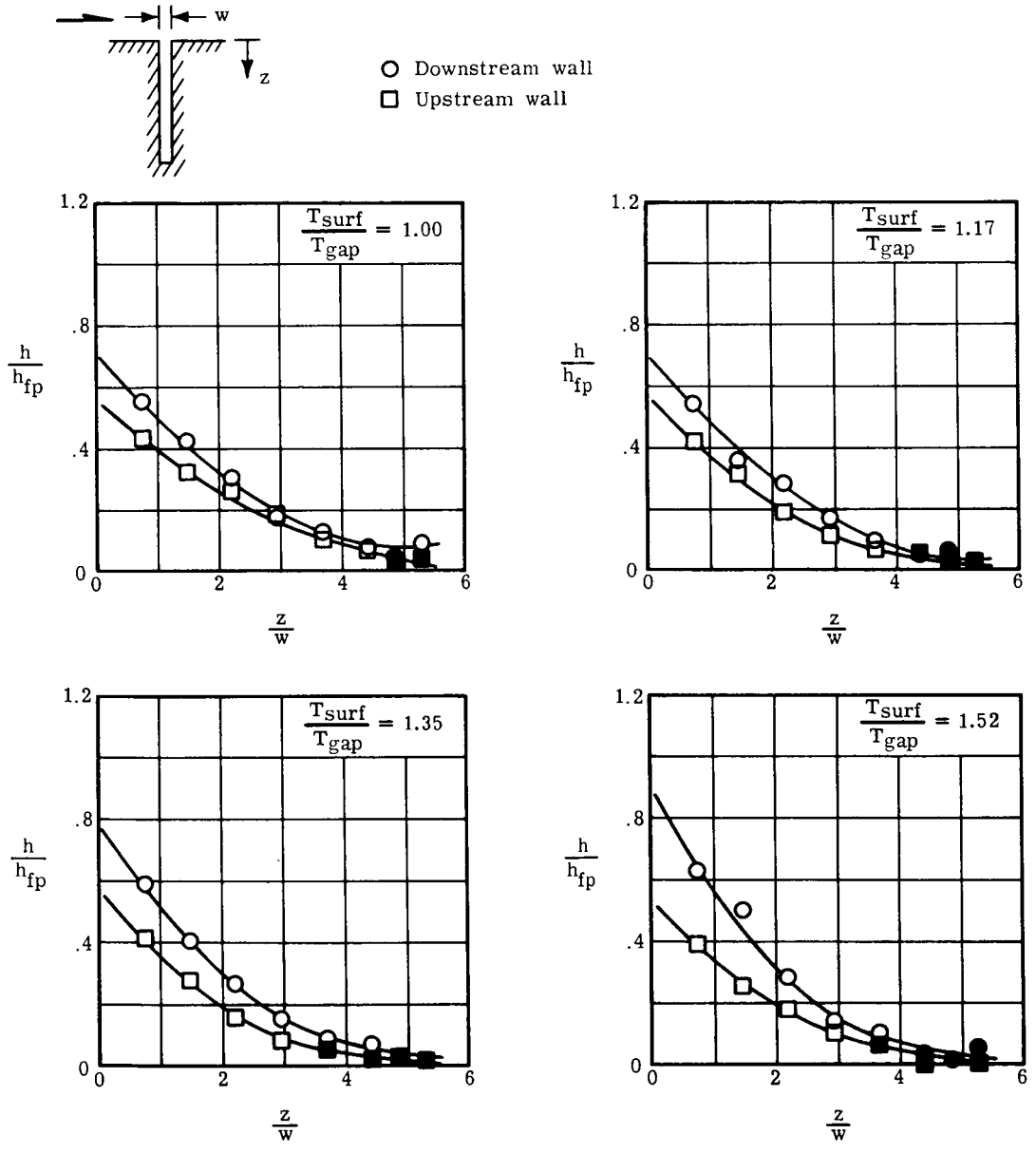

(b) $R_{\infty} = 3.26 \times 10^{6}\ m^{-1}$.

Figure 7.- Continued.

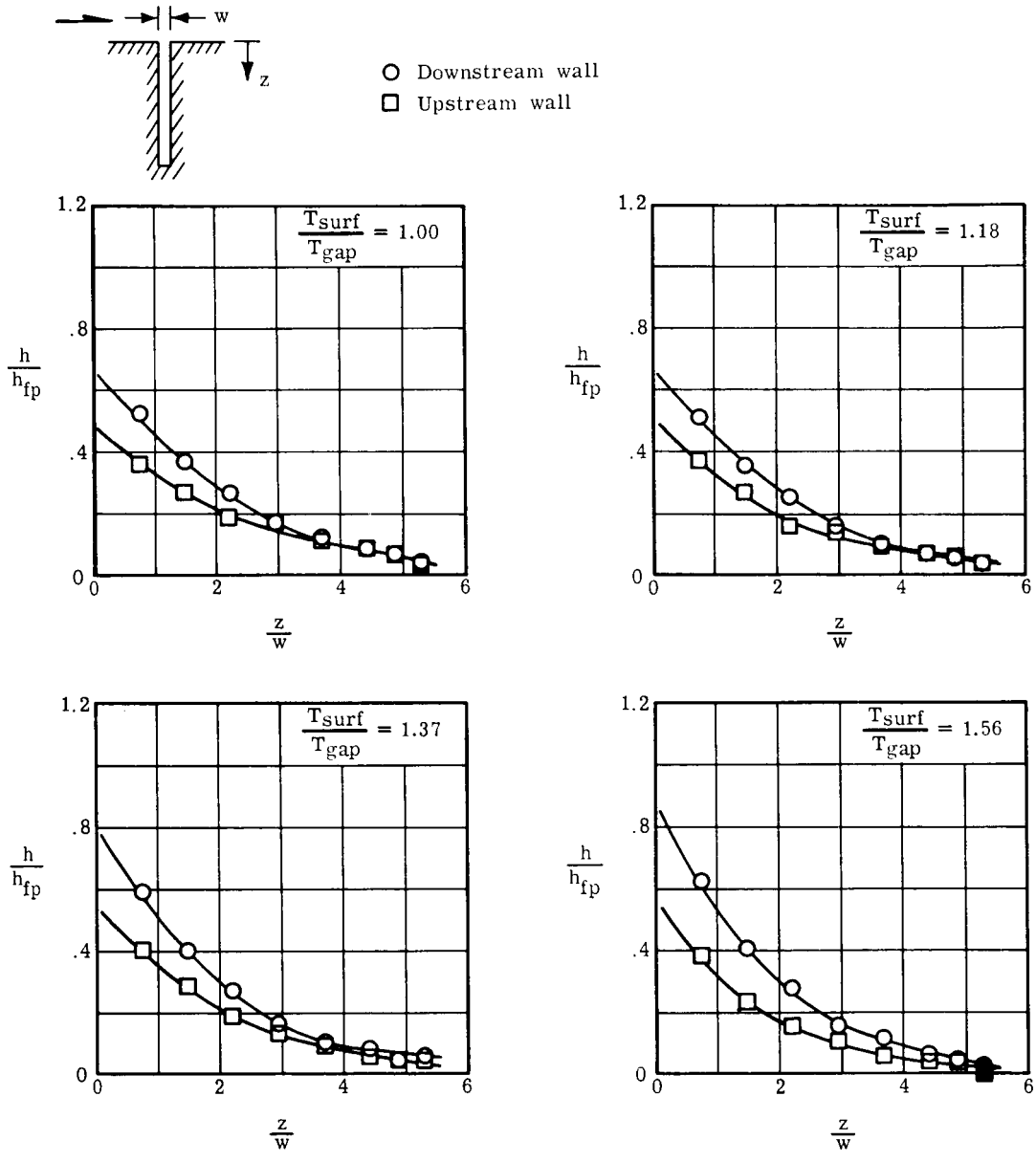

(c) $R_\infty = 7.76 \times 10^6\ m^{-1}$.

Figure 7.- Concluded.

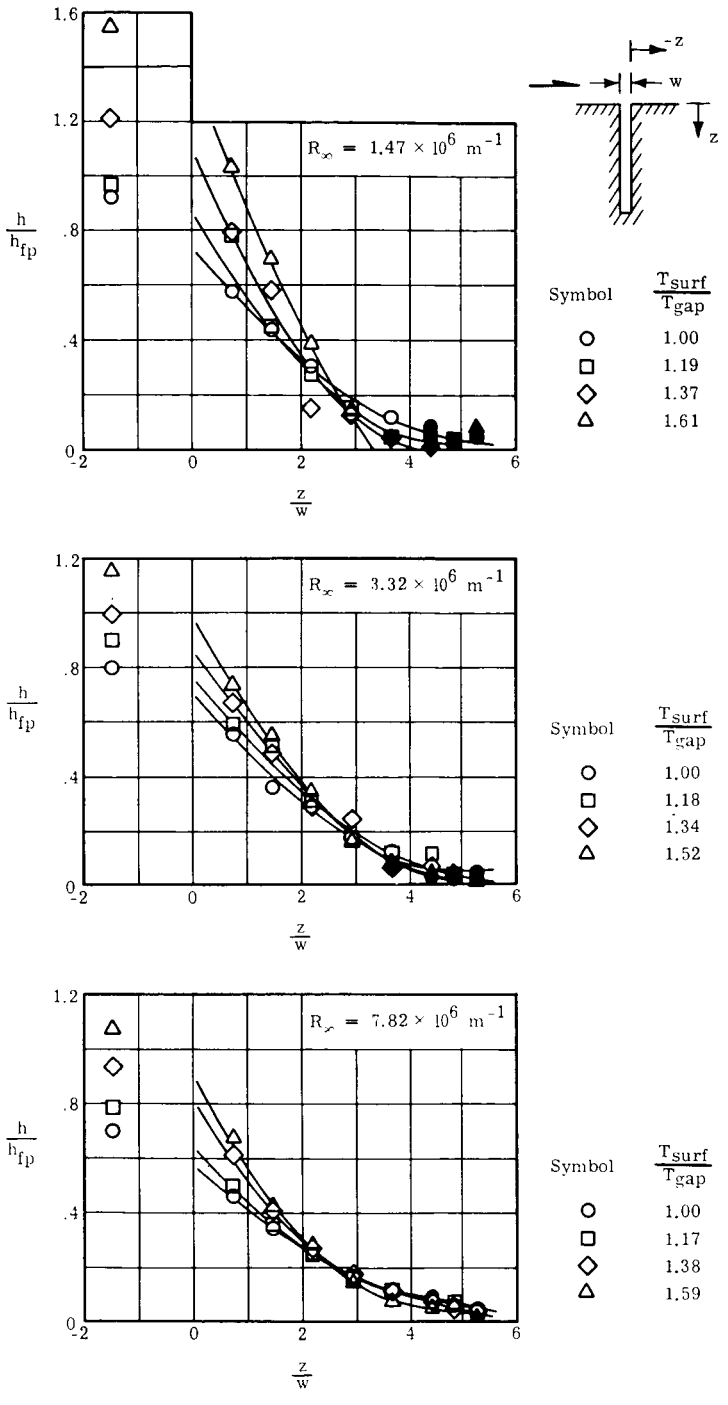

(a) $\Lambda = 0^{o}$.

Figure 8.- Measured heat transfer to the downstream gap wall.

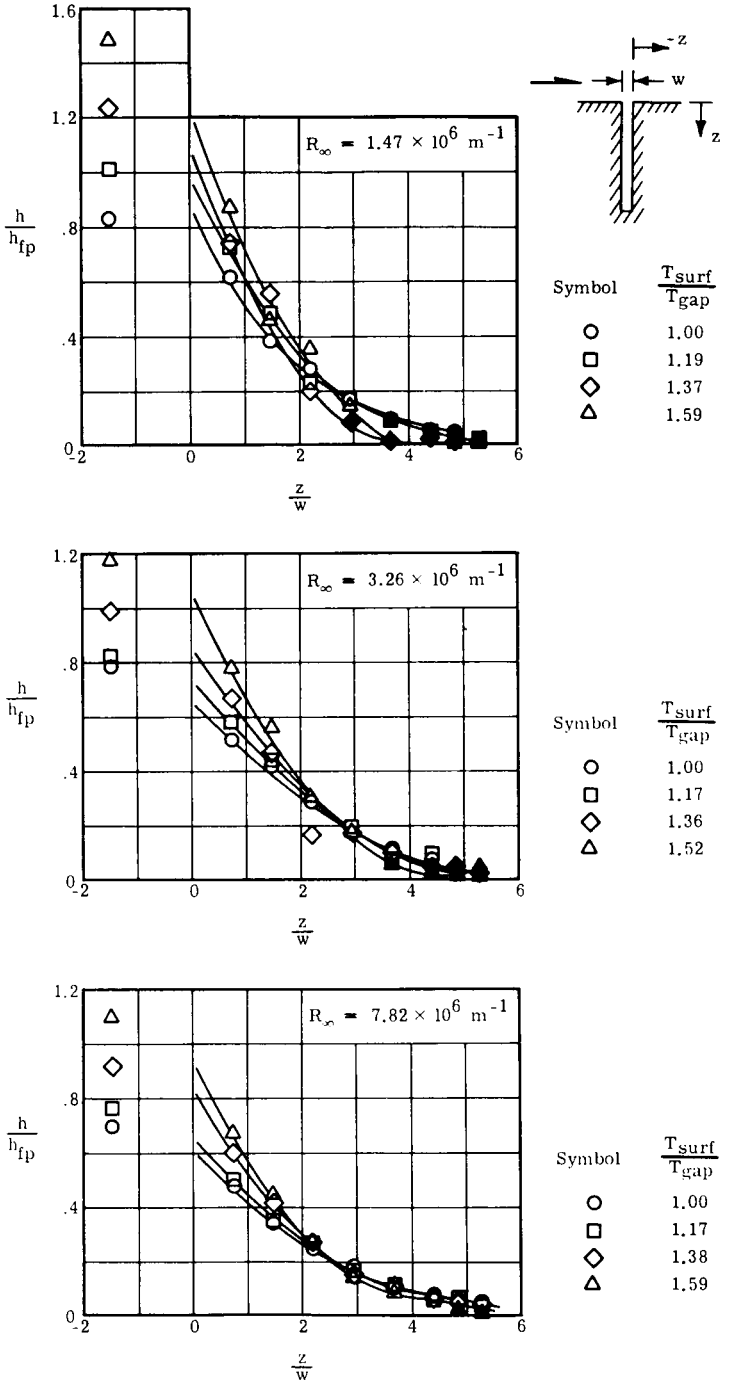

(b) $\Lambda = 30^{\circ}$.

Figure 8.- Continued.

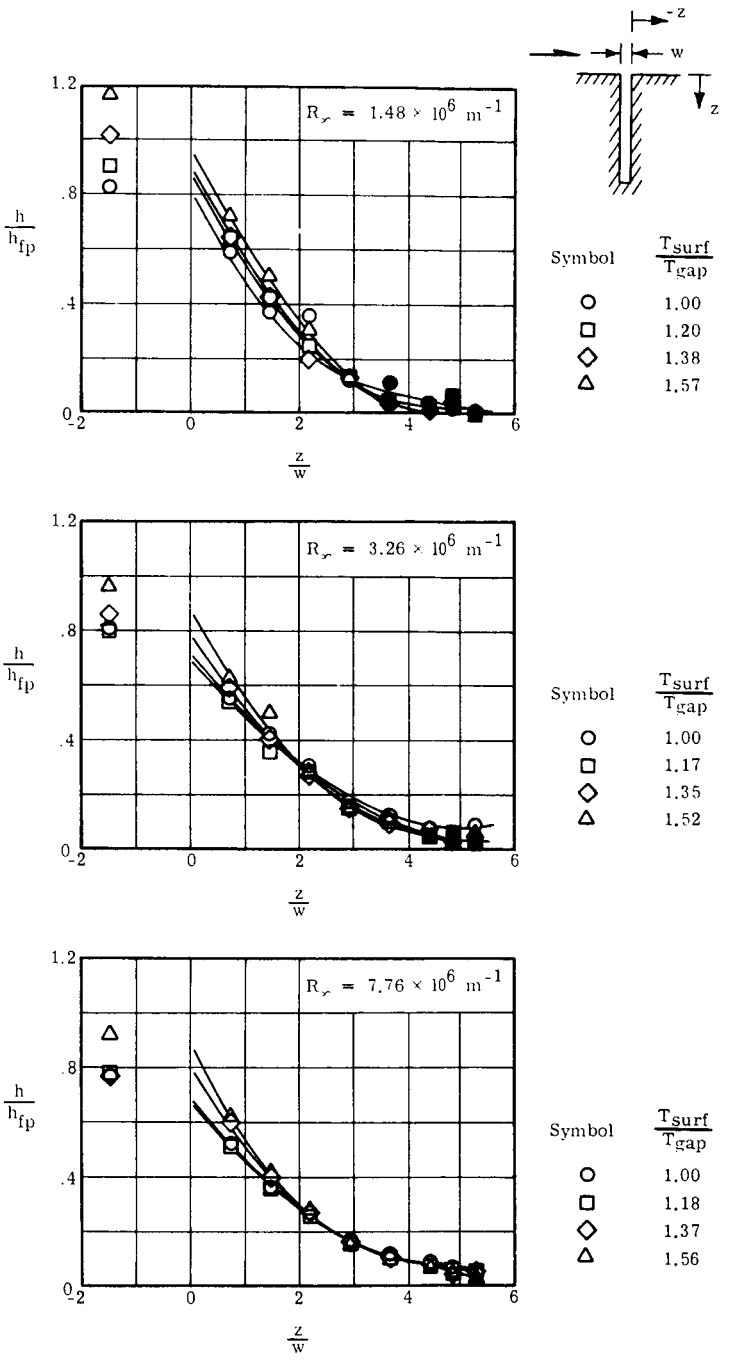

(c) $\Lambda = 60^{\circ}$.

Figure 8.- Concluded.

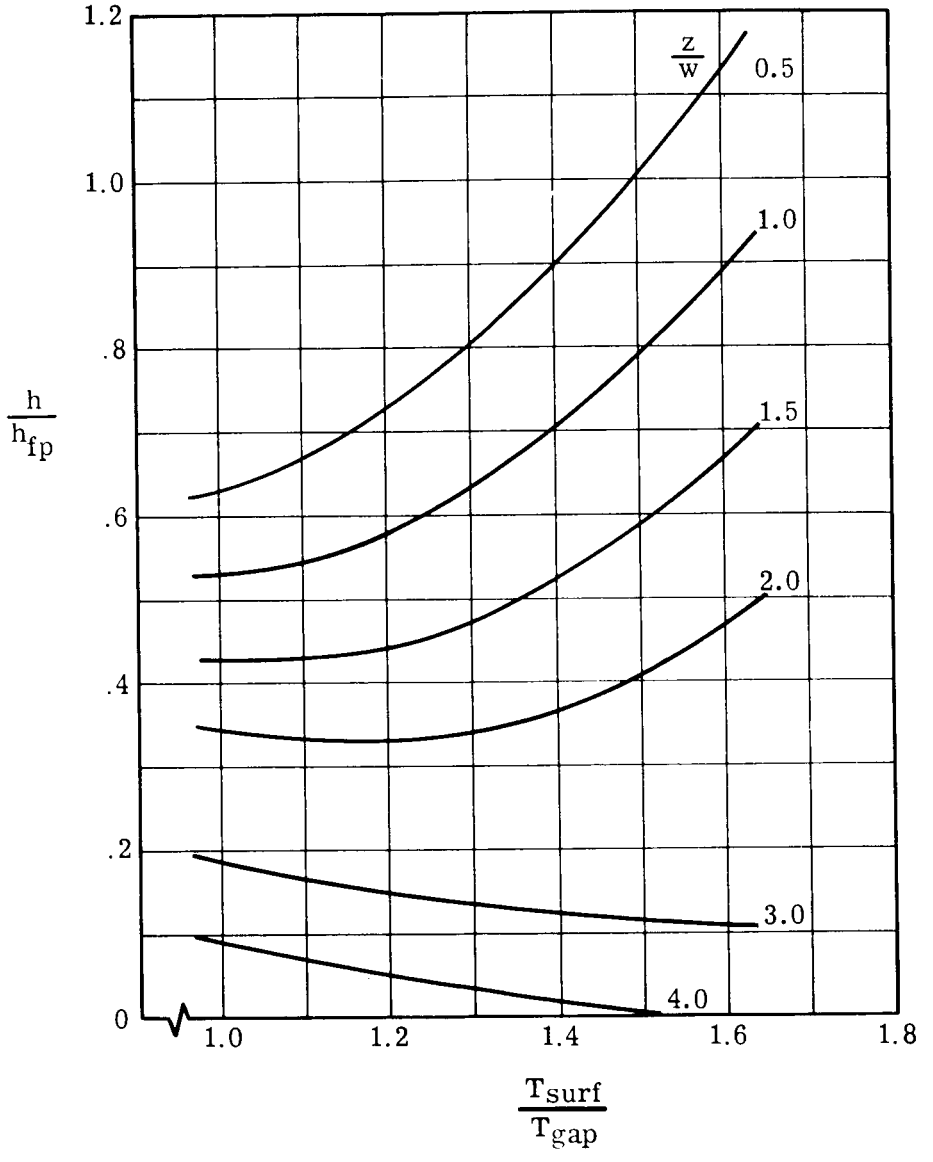

(a) $R_\infty = 1.47 \times 10^6\ m^{-1}$.

Figure 9.- Effect of ratio of surface temperature to gap-wall temperature on downstream gap-wall heat transfer. $\Lambda = 0^o$.

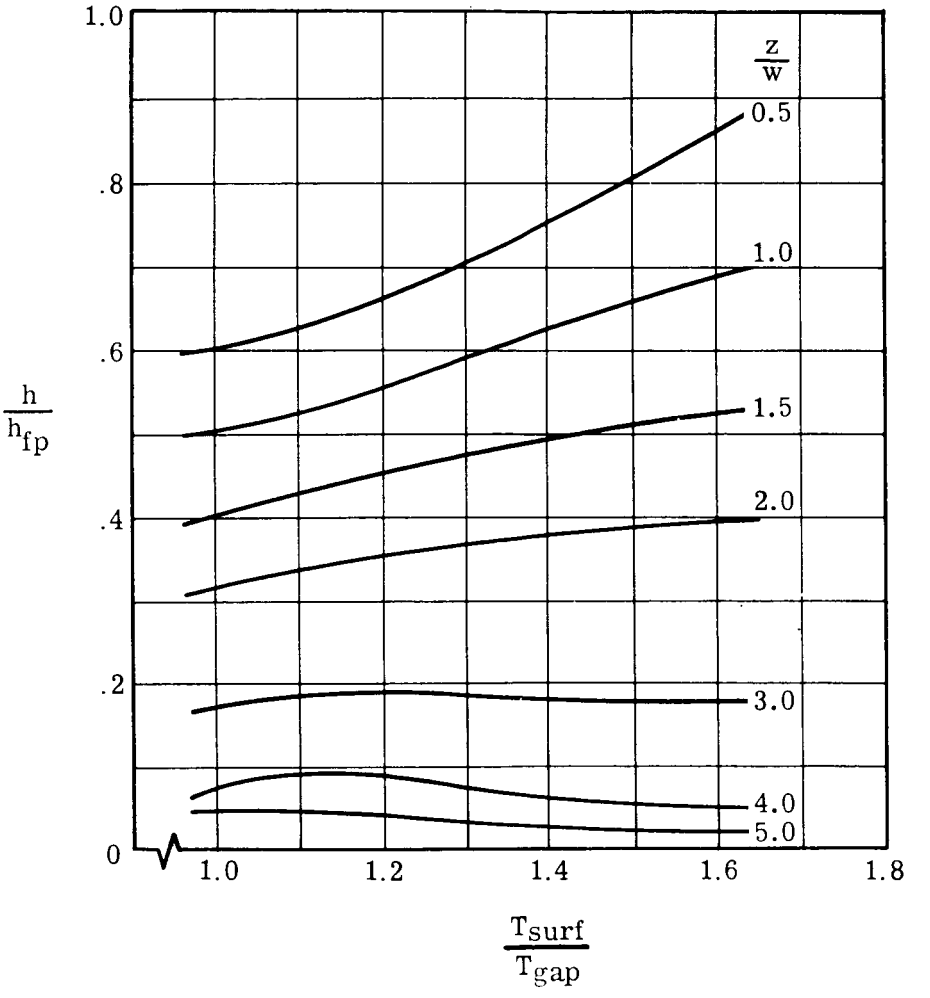

(b) $R_{\infty} = 3.32 \times 10^{6}\ m^{-1}$.

Figure 9.- Continued.

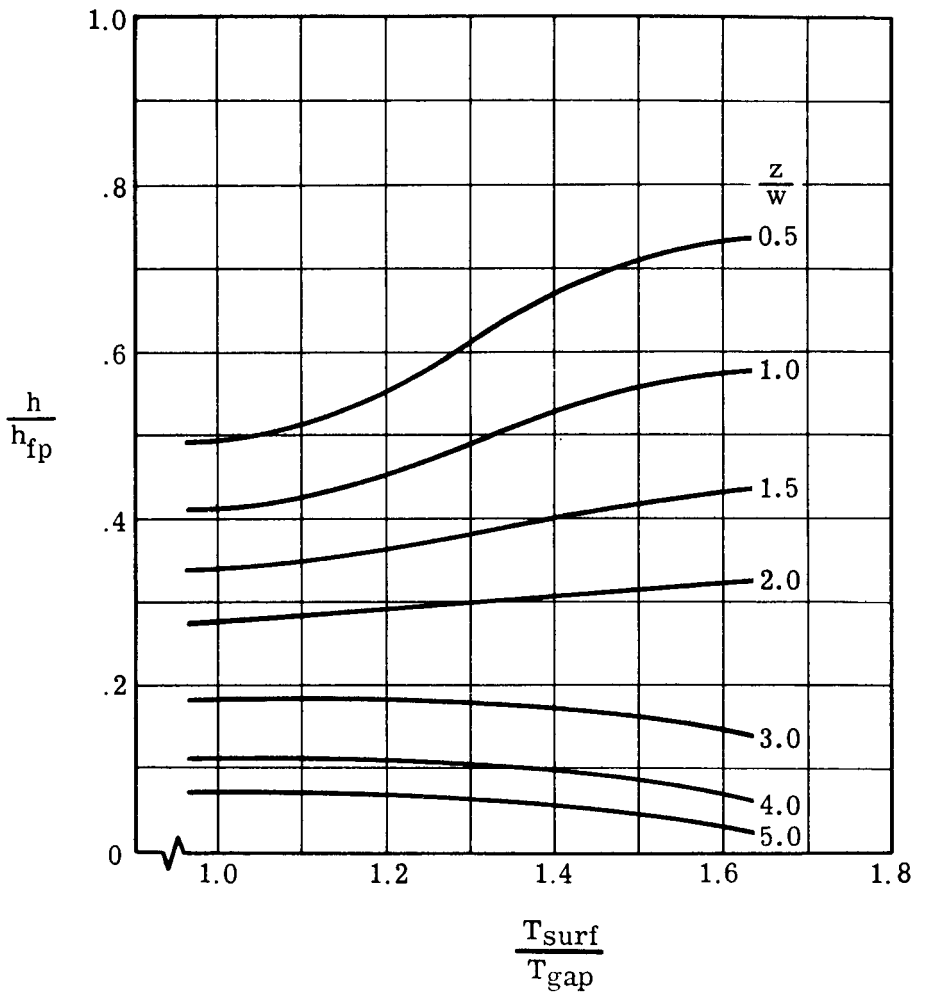

(c) $R_\infty = 7.82 \times 10^6\ m^{-1}$.

Figure 9.- Concluded.

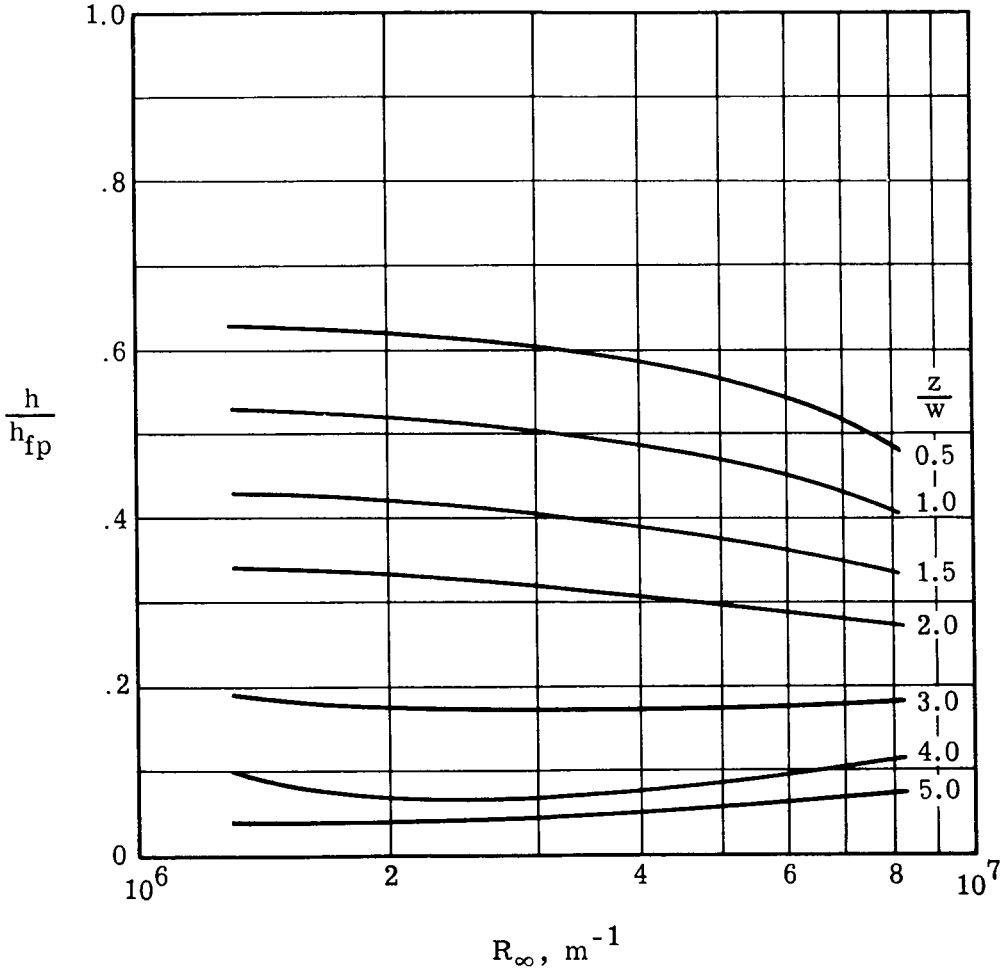

(a) $T_{surf}/T_{gap} = 1.00$.

Figure 10.- Effect of free-stream Reynolds number on downstream gap-wall heat transfer. $\Lambda = 0^{o}$.

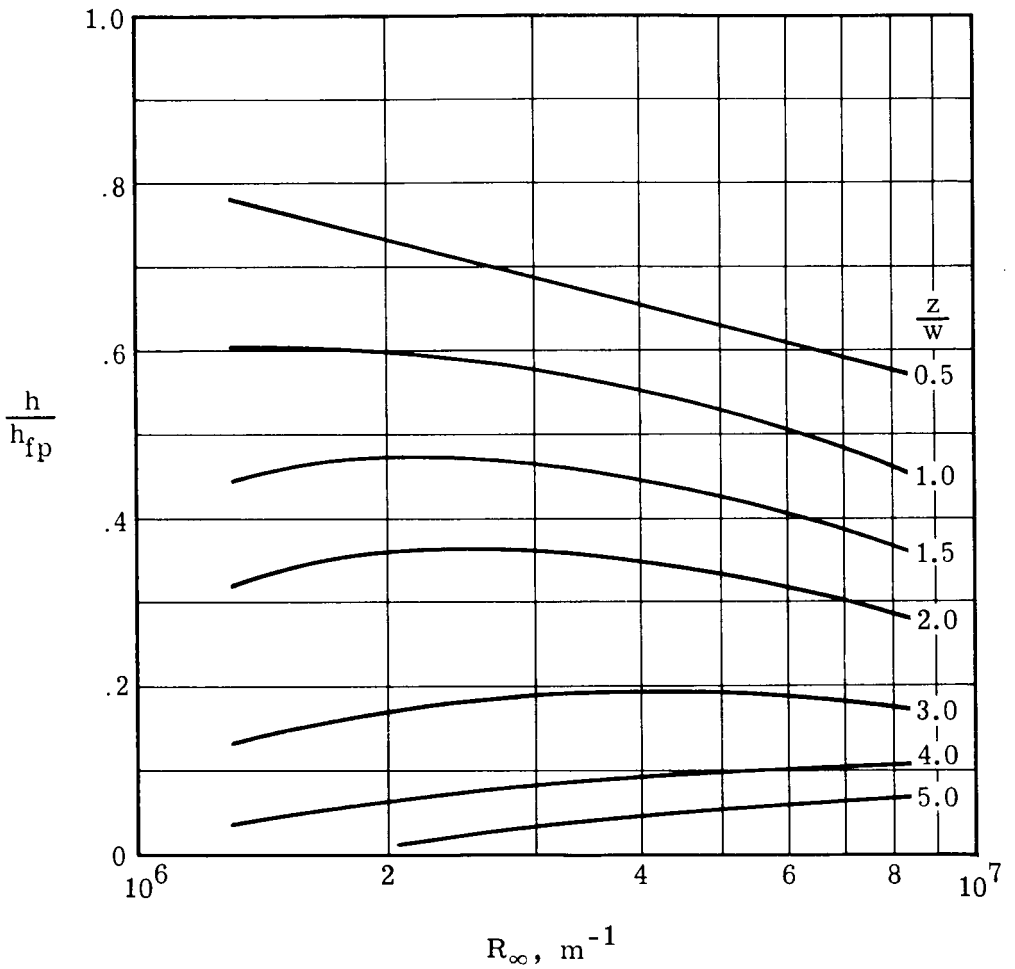

(b) $T_{surf}/T_{gap} = 1.25$.

Figure 10.- Continued.

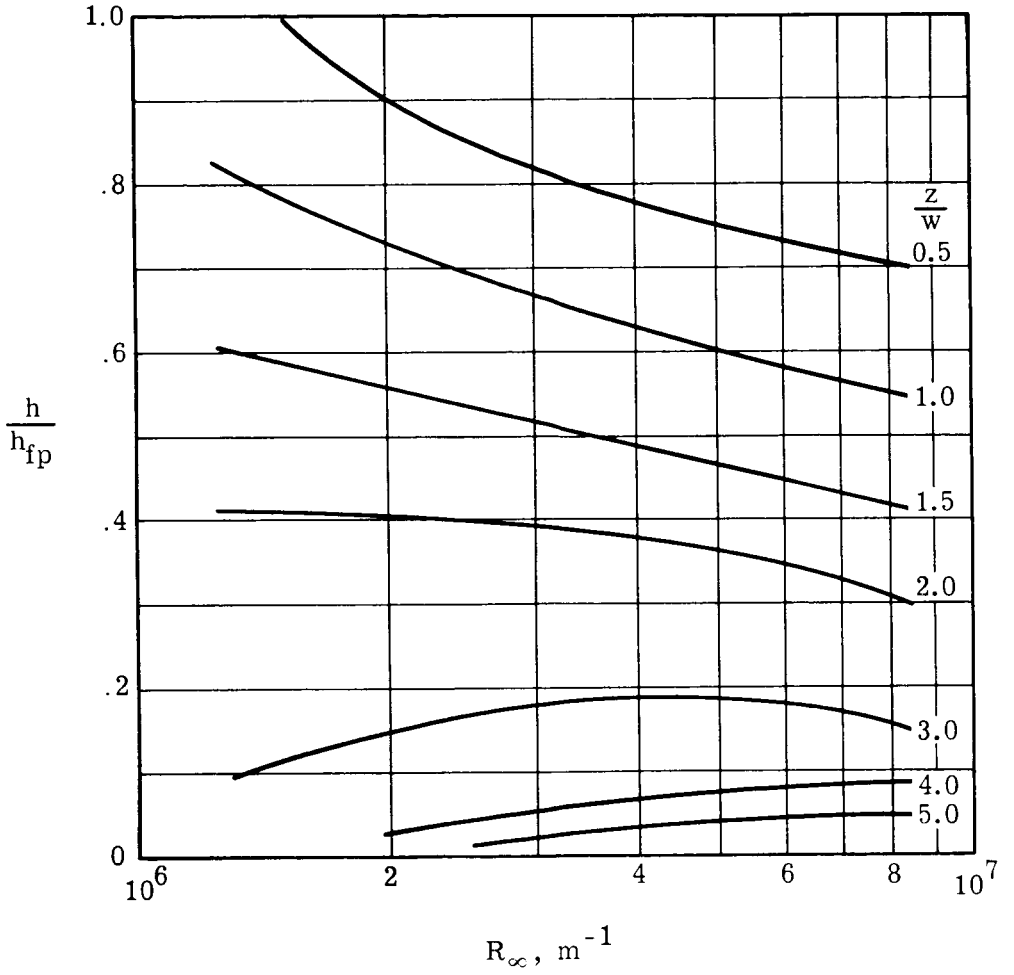

(c) $T_{surf}/T_{gap} = 1.50$.

Figure 10.- Concluded.

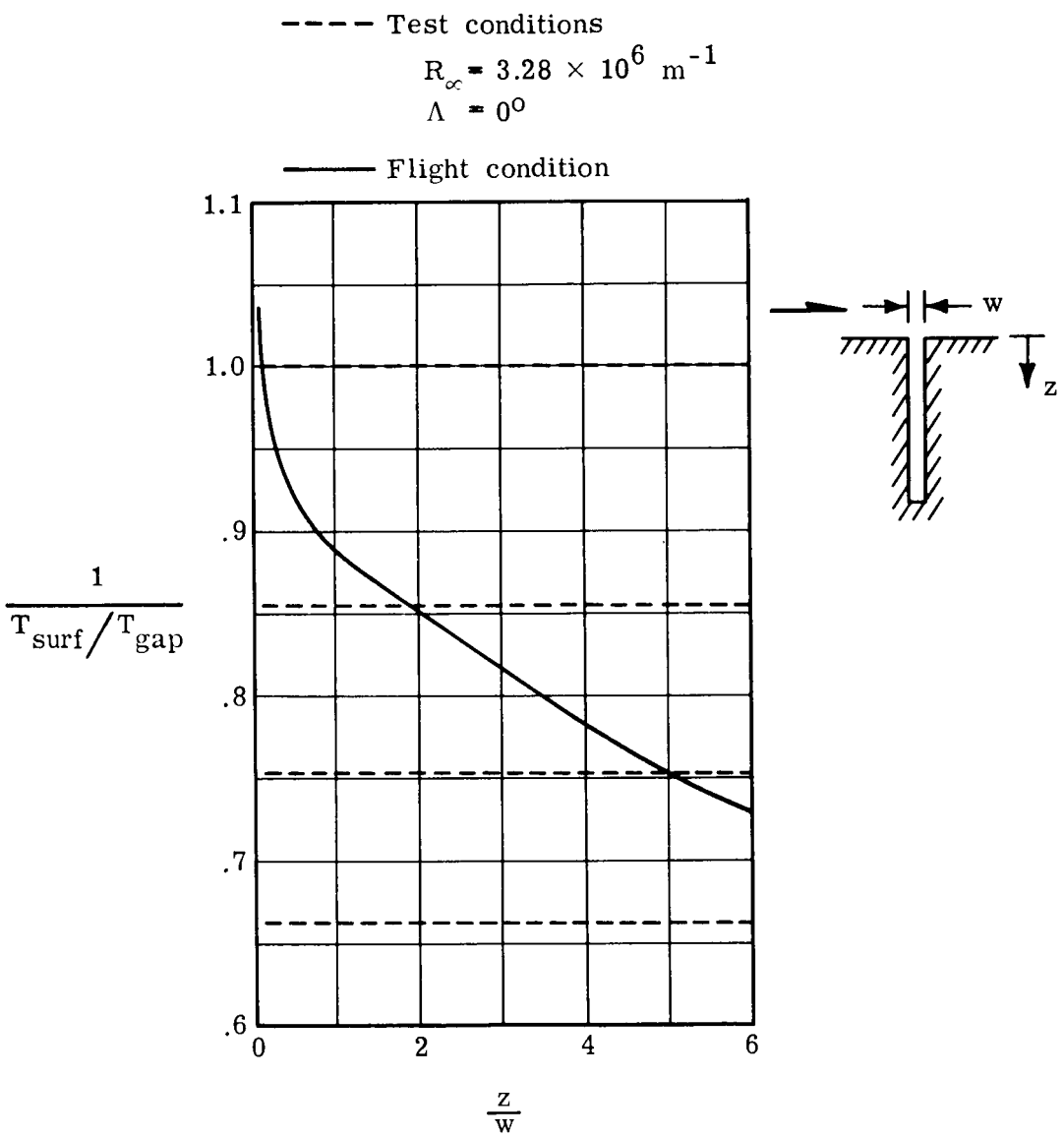

Figure 11.- Simulation of flight gap temperature ratio.

NASA-Langley, 1976 L-10766